PAPER

The preparation and application of a ROMP-type epoxy-functionalized norbornene copolymer and its hybrid alkaline anion exchange membranes†

Xiaohui He, [*a] Zhilong Han,[a] Yingping Yang,[a] Suli Wang,[a] Guangshui Tu,[a] Shengmei Huang,[ac] Feng Zhang[a] and Defu Chen[b]

A series of ROMP-type epoxy-functionalized norbornene copolymers named rP(BN/MGENB)-x, with different MGENB content, were synthesized by copolymerization of 5-norbornene-2-methylene butyl ether (BN) and 5-norbornene-2-epoxypropyl ether (MGENB) via ring-opening metathesis polymerization. The obtained rP(BN/MGENB)-49.2 showed the best molecular weight and processability performance for hybrid alkaline anion exchange membrane preparation. Based on this, cross-linked copolymer/silica hybrid alkaline anion exchange membranes, QrP(BN/MGENB-SiO$_2$-y) (y = 10, 20, 30 and 40 wt% TSPCA), were prepared by chemical reaction with N-trimethoxysilylpropyl-N,N,N-trimethylammonium chloride (TSPCA) and glutaric dialdehyde (GA). The effects of the TSPCA compositions on the mechanical properties, morphology, methanol resistance permeability, alkaline resistance stability, and ionic conductivity of the hybrid alkaline QrP(BN/MGENB-SiO$_2$-y) were investigated. QrP(BN/MGENB-SiO$_2$-10) exhibited the best comprehensive properties and ionic conductivity of all of the hybrid membranes. The ionic conductivity increased obviously with a rise in temperature, and values of 9.7×10^{-3} S cm^{-1} at 30 °C and 41×10^{-3} S cm^{-1} at 80 °C were obtained. A membrane electrode assembly (MEA) fabricated using QrP(BN/MGENB-SiO$_2$-10) was also tested in a direct methanol fuel cell, and a maximum open circuit voltage (OCV) of 0.95 V and a current density of 96.7 mW cm^{-2} at a peak power density of 42.6 mW cm^{-2} at 80 °C were achieved.

Introduction

Over the past several decades, the critical nature of the petrochemical resources shortage issues has led to a significant increase in the demand for renewable energy technologies.[1] As an important component of direct methanol fuel cells, anion exchange membranes (AEMs) have attracted a great deal of attention – especially concerning the use of non-noble metals (such as nickel, silver and cobalt) – due to the superiority of direct methanol fuel cells to proton exchange membrane (PEM) fuel cells.[2–4] To date, benzyltrimethylammonium (BTMA) and alkyltrimethylammonium cations have been employed in AEMs with polysulfones,[5] polystyrene (PS),[6] polyvinylalcohol (PVA),[7] and polynorbornene (PNB).[8–10]

In addition, cationic groups such as imidazolium,[11] and quaternary ammonium[12] have also been screened for developing stable and efficient AEMs. However, the backbone of the quaternized polymer, which contained a heterocyclic ring or benzyl ring, was usually degraded in alkaline conditions.[13] An ideal anion exchange membrane should possess the advantages of excellent mechanical properties, good dimensional stability, high hydroxide conductivity and adequate hydroxide stability. The stability of AEMs is still an important parameter for practical fuel cell applications.[14,15] To achieve the above objectives, a cross-linking strategy has been applied in the design of the polymer architecture to obtain mechanically robust AEMs with improved stability.

Polynorbornene (PNB) has been used for AEM polymer matrix preparation.[16,17] Membranes based on addition-type polynorbornene (aPNB)[18] that were prepared via vinyl-addition polymerization had poor performance in their processing properties, conductivity, and water uptake.[19] To improve the processing property, conductivity and hydrophilicity of the aPNB, a simple but useful measure taken was to design and prepare polynorbornene-based hybrid membranes with flexible backbones or polar functional groups. ROMP-type polynorbornene (rPNB)[20] could be prepared with a high molecular weight at normal temperatures and pressures and exhibited

[a]School of Materials Science and Engineering, Nanchang University, 999 Xuefu Avenue, Nanchang 330031, China. E-mail: hexiaohui@ncu.edu.cn

[b]School of Civil Engineering and Architecture, Nanchang University, 999 Xuefu Avenue, Nanchang 330031, China

[c]School of Materials Science and Engineering, Nanchang Hangkong University, Nanchang 330063, China

excellent processability. In addition, a cross-linked AEM was developed by Coates and co-workers, who employed ring-opening metathesis polymerization (ROMP) of a tetraalkylammonium-functionalized norbornene with dicyclopentadiene (DCPD). The resulting cross-linked fully hydrated membrane demonstrated high hydroxide conductivities, with a conductivity of 18 mS cm^{-1} at 20 °C.[21] In epoxy-functionalized norbornene, the epoxy group on the monomer endows the polymer with excellent processability. In addition, as with the epoxy group which is an active functional group, a mass of other significant functional groups could be grafted on easily. Therefore, copolynorbornenes obtained by copolymerization of epoxy-functionalized norbornene with another norbornene monomer functionalized with an alkoxy group, amine group or siloxane group, had excellent heat resistance,[22] weatherability,[23] hydrophilicity, etc.[24]

By adding inorganic particles, such as α-Al$_2$O$_3$,[25] ZrO$_2$,[26] SiO$_2$,[27] bentonite,[28] and TiO$_2$ (ref. 29) into the polymer matrix to prepare hybrid membranes, the ionic conductivity and chemical stability can be enhanced obviously. Many methods have been applied to introduce inorganic particles into organic networks, such as blending,[30] sol–gel methods,[31–34] and in situ polymerization.[35] In hybrid membranes, the organic and inorganic components should be combined with each other completely. However, hybrid membranes prepared by physical mixing with inorganic particles have shown poor swelling stability. To synthesize AEMs, an effective and simple way is via chemical reactions grafted on polymer chains by using silica with quaternary ammonium groups. In addition, high tensile strength and elastic moduli of hybrid membranes could be obtained by using a sol–gel method to further form cross-linked networks.

In this work, ROMP-type epoxy-functionalized norbornene copolymers, named rP(BN/MGENB)-x with different MGENB content, were synthesized by copolymerization of 5-norbornene-2-methylene butyl ether (BN) and 5-norbornene-2-epoxypropyl ether (MGENB) via ring-opening metathesis polymerization catalyzed by Grubbs' 1st catalyst. Copolymer/silica hybrid alkaline anion exchange membranes, QrP(BN/MGENB-SiO$_2$-y), were further prepared via chemical reactions of rP(BN/MGENB)-49.2, N-trimethoxysilylpropyl-N,N,N-trimethylammonium chloride (TSPCA), and glutaraldehyde (GA). The mechanical properties, morphology, methanol permeability, alkaline stability, and ionic conductivity, as well as the single cell performance of the hybrid membranes were investigated to assess their suitability as alkaline anion exchange membranes for direct methanol fuel cell (DMFC) application.

Experimental

Materials

N-Trimethoxysilylpropyl-N,N,N-trimethylammonium chloride (TSPCA), glutaraldehyde (GA), 5-norbornene-2-methanol, sodium hydroxide (NaH), and Grubbs' 1st catalyst [Cl$_2$(PCy$_3$)$_2$-Ru=CH–Ph] were used from Energy Chemical Co. Ltd. Epoxy chloropropane, 2-bromobutane, and hydrochloric acid were provided by Tianjin Damao Chemical Co. Ltd. Tetrahydrofuran,

toluene, hexane and dichloromethane were distilled from sodium and benzophenone under nitrogen.

Synthesis of 5-norbornene-2-methylene glycidyl ether (MGENB)

Monomer MGENB was synthesized by the following procedure: 21 mL (0.67 mol) 5-norbornene-2-methanol was dissolved in THF, and 8 g (0.2 mol) NaH was added into a Schlenk, which was placed in an ice water bath for 3 h. The mixture was stirred at room temperature for 5 h, then 18.5 mL (0.2 mol) epoxy chloropropane was added into the Schlenk under −90 °C for 4 h. After being stirred vigorously for 24 h at room temperature, the product was purified by column chromatography [SiO$_2$ with an eluent of petroleum ether–ethyl acetate (v/v = 4/1)] and distilled at reduced pressure. The synthesized monomer was dried over Na and vacuum-distilled before copolymerization.

Synthesis of 5-norbornene-2-methylene butyl ether(BN)

Monomer BN was synthesized according to the procedure reported by Liu et al.[36]

Synthesis of ROMP-type epoxy-functionalized norbornene copolymer

ROMP-type epoxy-functionalized norbornene copolymers rP(BN/MGENB)-x were prepared as shown in Scheme 1. All of the copolymerizations were performed under a nitrogen atmosphere, toluene was distilled from sodium prior to use. Copolymerizations of BN and MGENB (BN/MGENB = 7/3, 6/4, 5/5, and 4/6 in molar ratio) were carried out using Grubbs' 1st catalyst [Cl$_2$(PCy$_3$)$_2$Ru=CH–Ph] in a 100 mL Schlenk with magnetic stirring. [Cl$_2$(PCy$_3$)$_2$Ru=CH–Ph] (100 mg, 0.11 mmol) was dissolved in 10 mL toluene, and then the mixture was stirred at 30 °C for 4 h before the reaction was terminated by adding ethyl vinyl ether. The polymer solution was precipitated in hexanes, purified, and dried under vacuum. The obtained copolymer rP(BN/MGENB)-49.2 was chosen to be the polymer matrix material for the preparation of the copolymer/silica hybrid membranes.

Copolymer/silica hybrid membrane preparation

The chosen rP(BN/MGENB)-49.2 (2 g) was divided into four equal parts and each part was dissolved in THF till the polymer completely dissolved in a Schlenk at room temperature, then a different content of N-trimethoxysilylpropyl-N,N,N-trimethylammonium chloride (TSPCA) was added into the above Schlenk for 1 h at 30 °C (copolymer/TSPCA = 9 : 1, 8 : 2, 7 : 3, and 6 : 4 mass ratio). An aqueous solution of HCl (0.1 mL, 1 mol L^{-1}) was used to control the pH value of the solution. 0.05 mL glutaraldehyde (GA) was added for further cross-linking at 30 °C for 8 h. After that, the homogenous solution was cast onto clean PTFE molds and dried at 50 °C to obtain hybrid membranes. The molds were soaked in an aqueous solution of sodium hydroxide to obtain flaxen and transparent hybrid membranes. The obtained hybrid membranes were dried under vacuum at 30 °C for 48 h and defined as QrP(BN/MGENB-SiO$_2$-y)
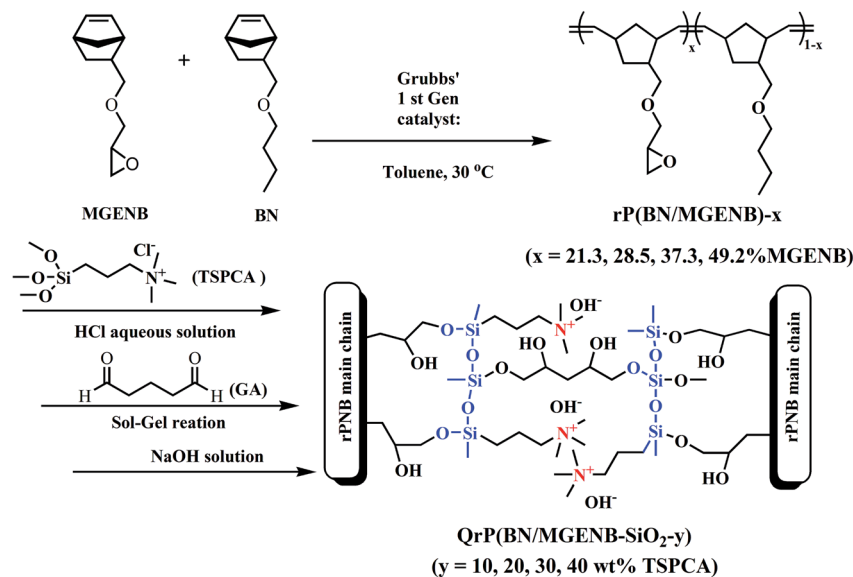
Scheme 1 The synthesis route of ROMP epoxy-functionalized norbornene copolymer and its hybrid anion exchange membranes.

(y = 10, 20, 30 and 40 wt% TSPCA). The route for the hybrid membranes' syntheses is shown in Scheme 1.

^{1}H NMR and ^{13}C NMR spectra characterization

^{1}H NMR and ^{13}C NMR spectra were measured on an ARX600 Nuclear Resonance Spectrograph by Bruker. Chloroform-d was used as solvent. The monomers, copolymers, and copolymer/silica hybrid membrane were identified from their respective ^{1}H NMR and ^{13}C NMR spectra.

FT-IR spectroscopy characterization

Fourier transform infrared attenuated total reflection (FTIR-ATR) spectra were obtained from dried copolymer/silica hybrid membrane samples (IRPrestige-21 FT-IR spectrometer Shimadzu) in the range of 4000–400 cm^{-1}. The monomer and copolymer were identified from the FT-IR spectra.

Thermal analyses and mechanical properties test

A TGA-7 Perkin Elmer thermal analyzer was used to determine the thermal stability with a heating rate of 10 °C min^{-1}. An MTS CMT8502 was used to test the mechanical properties of the copolymer/silica hybrid membrane.

Microscopic characterizations

The morphology of the prepared copolymer/silica hybrid membrane was observed by transmission electron microscopy (TEM, Tecnai G220 S-TWIN). The sample was dissolved in THF and dropped onto a 200-mesh copper net. A Hitachi S-3000N was used to record the elements in the membrane. The surface and cross section morphology of the membrane were investigated by scanning electron microscopy (ESEM, FEI Quanta 200).

Gel permeation chromatography test

Gel permeation chromatography (GPC) was conducted using a Breeze Waters system equipped with a Rheodyne injector, a 1515 isocratic pump, and a waters 2414 differential refractometer by using polystyrene as the standard and tetrahydrofuran (THF) as the solvent.

Water uptake and methanol permeability measurements

The water uptake (WU) was measured via the following steps: all of the copolymer/silica hybrid membranes were cut to 40 × 10 mm in size and immersed in deionized water for 48 h at 80 °C. The water uptake η (%) was determined by the following equation:

$$\eta_{\text{w}} = \frac{m_{\text{w}} - m_{\text{d}}}{m_{\text{d}}} \times 100\%$$

The methanol permeability of the copolymer/silica hybrid membrane was measured using liquid permeation equipment with two compartments. The membrane was cut into a round piece and sandwiched between two compartments which contained 6 M aqueous methanol solution and deionized water, respectively. The two compartments were continuously stirred during testing. The concentration of methanol in the deionized water was periodically determined by gas chromatography (GC). The methanol permeability was calculated using the following equation:

$$p = \frac{V_{\text{m}}l}{AC_{\text{m}}} \frac{C_{\text{w}}}{(t - t_0)}$$

where A (cm^2) is the cross sectional area of the membrane, l (cm) is the thickness of the membrane, and V_{m} is the volume of the permeated reservoirs. C_{w} and C_{m} (mol L^{-1}) are the methanol concentrations in the donor and receptor reservoirs, respectively.

Ion-exchange capacity (IEC), ionic conductivity and alkaline stability tests

The copolymer/silica hybrid membrane was soaked in a 50 mL HCl (0.01 mol L^{-1}) aqueous solution for 24 h. Then, an aqueous solution of NaOH (0.01 mol L^{-1}) was titrated and methyl orange was used as an indicator. The *IEC* parameter (mmol g^{-1}) was calculated using the following equation:

$$IEC = \frac{C_{HCl}V_{HCl} - C_{NaOH}V_{NaOH}}{m}$$

The ionic conductivities (δ) of the copolymer/silica hybrid membranes QrP(BN/MGENB-SiO$_2$-y) were evaluated by an AC impedance test using a CHI660 electrochemical workstation. The compartments were connected to each other with fasteners, with a hole between the two compartments. Then, 50 mL NaOH (1 M) aqueous solution was poured into the compartments, the resistance of the solution was measured as R_1. After that, the sample was sandwiched between the two compartments, 50 mL NaOH (1 M) aqueous solution was poured into the compartments, and the resistance of the solution was measured as R_2. The ionic conductivity (δ) of the membrane was calculated using the following equation:

$$\delta = \frac{l}{(R_2 - R_1)A}$$

The alkaline stability of the copolymer/silica hybrid membrane was tested by soaking it in a 6 M NaOH aqueous solution, the anion conductivity of the membrane was recorded every 24 h using a CHI660 electrochemical workstation. The δ value of the membrane was calculated using the above equation.

Single cell performance test

The copolymer/silica hybrid membrane was cut to a size of 25 × 3 mm. A Fuel Cell Test Station (BT2000, Arbin Co.) was used to test the current density, open circuit voltage, and peak power density of the copolymer/silica hybrid membrane.

Results and discussion

ROMP-type epoxy-functionalized norbornene copolymer

A series of ROMP-type epoxy-functionalized norbornene copolymers rP(BN/MGENB)-x and their hybrid alkaline anion exchange membranes QrP(BN/MGENB-SiO$_2$-y) were synthesized as shown in Scheme 1.

The structures of rP(BN/MGENB)-x with different MGENB content were characterized by ^{1}H NMR spectroscopy (Fig. 1). It was proved that the copolymers were prepared *via* ring-opening metathesis polymerization due to the disappearance of peaks around 6.0 ppm and the appearance of peaks around 5.3 ppm. The peaks at 2.58 and 2.76 ppm could be assigned to the hydrogen corresponding to the H^{11} in the MGENB monomer.

The ^{13}C NMR spectra of the ROMP-type epoxy-functionalized norbornene copolymers are shown in Fig. 2. The resonance

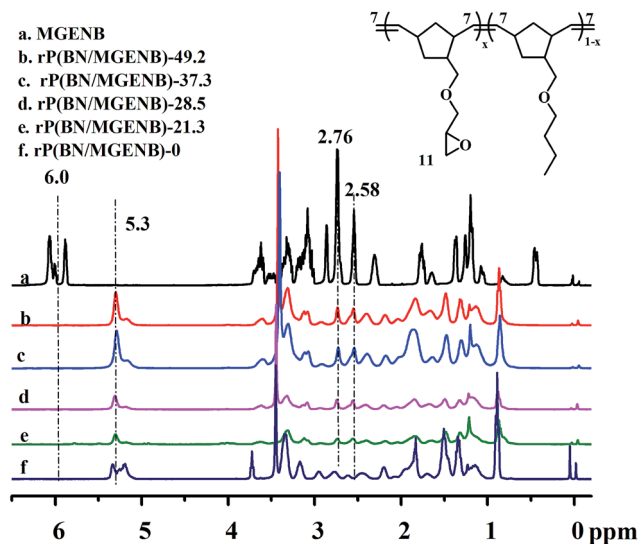**Fig. 1** ^{1}H NMR spectra of ROMP-type epoxy-functionalized norbornene copolymers: (a) rP(BN/MGENB)-100, (b) rP(BN/MGENB)-49.2, (c) rP(BN/MGENB)-37.3, (d) rP(BN/MGENB)-28.5, (e) rP(BN/MGENB)-21.3, and (f) rP(BN/MGENB)-0.

peaks appearing between 69 and 74 ppm could be attributed to the methene carbons (C5/C6/C7/C8). The peaks at 51 and 45 ppm were assigned to the epoxy group methene carbons that correspond to C3 and C4. The appearance of C=C bond characteristic peaks at 130 and 132 ppm owing to the ROMP-type polynorbornene structures further imply that the copolymerization of BN and MGENB catalyzed by Grubbs' 1st catalyst was carried out *via* ring-opening metathesis polymerization.

In Fig. 3(a), major FT-IR absorptions of MGENB appearing at 1252, 1100, 929, 906 and 720 cm^{-1} were observed. A wide absorption band around 1100 cm^{-1} in Fig. 3(b) and (c) was assigned to Si–O–Si vibrations and C–O–Si vibrations. In Fig. 3(c), a wide absorption band around 3450 cm^{-1} was
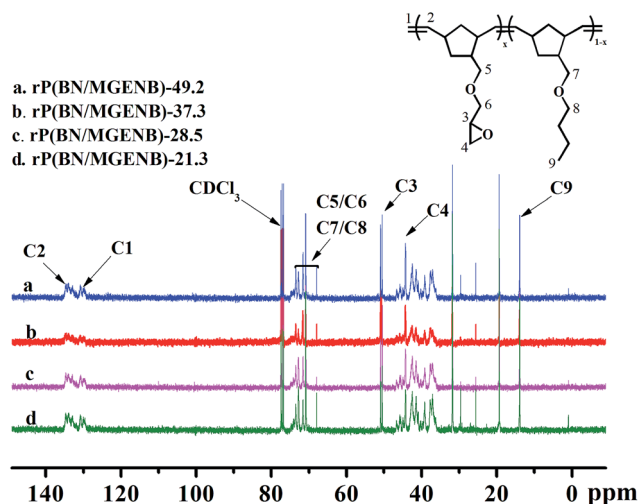

Fig. 2 ^{13}C NMR spectra of ROMP-type epoxy-functionalized norbornene copolymers: (a) rP(BN/MGENB)-49.2, (b) rP(BN/MGENB)-37.3, (c) rP(BN/MGENB)-28.5, and (d) rP(BN/MGENB)-21.3.
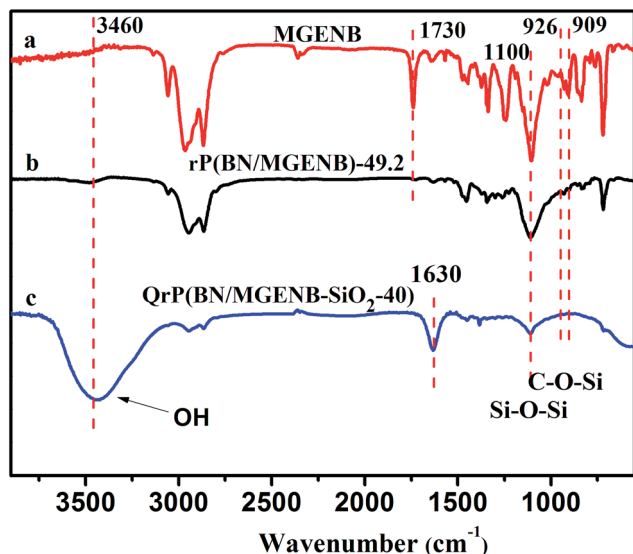
Fig. 3 FTIR spectra of (a) monomer MGENB, (b) copolymer rP(BN/MGENB)-49.2, and (c) the copolymer/silica hybrid membrane QrP(BN/MGENB-SiO$_2$-40).

assigned to –OH in the hybrid membrane, which indicated that a cross-linked network was formed successfully.

The epoxy-functionalized norbornene was introduced to the copolymer rP(BN/MGENB)-x, and the peaks at 2.58 and 2.72 ppm could be assigned to the hydrogen corresponding to the H^{11} in the MGENB. The content of MGENB in copolynorbornene could be carefully controlled by adjusting the monomer feed ratios, BN/MGENB = 7/3, 6/4, 5/5, and 4/6, and were calculated to be (a) 21.3%, (b) 28.5%, (c) 37.3%, and (d) 49.2% by the following equation:

$$\frac{S_a}{S_a + S_b} = \frac{x}{1-x}$$

where S_a was the peak of 2.58 ppm, S_b was the peak of 5.3 ppm, x was set as the content of MGENB, and the content of BN was set as $1 - x$.

The epoxy-functionalized norbornene copolymers, rP(BN/MGENB)-x, were characterized by GPC (Table S1 and Fig. S1†). The molecular weights (M_w) of the obtained copolymers were all in the scale of 10^4 and they had narrow dispersity. The GPC data indicated that the epoxy group in the copolymer had no effect on the catalytic activity, the molecular weight increased from 49 039 to 64 876 g mol^{-1} and the polymer dispersity index decreased from 1.69 to 1.62 when the MGENB content increased from 21.3 to 49.2%.

The solubility of the epoxy-functionalized norbornene copolymers rP(BN/MGENB)-x (Table S2†) also indicated that the epoxy group was conserved in all of the copolymers. The rP(BN/MGENB)-49.2 exhibited the highest M_w and the best processing performance.

Copolymer/silica hybrid membrane

The cross-linked copolymer/silica hybrid alkaline anion exchange membranes QrP(BN/MGENB-SiO$_2$-y) were obtained by

chemical reaction of rP(BN/MGENB)-49.2, TSPCA, and GA *via* a sol–gel method under an acid environment. All of the obtained copolymer/silica hybrid membranes were homogeneous, flexible, and dark brown with a thickness of around 160 μm. Photos of the hybrid membranes and their corresponding solutions before casting are presented in Fig. 4.

As a representative copolymer/silica hybrid membrane, QrP(BN/MGENB-SiO$_2$-40) was characterized by ^{1}H NMR spectroscopy (Fig. S2†). The peaks at 2.58 and 2.72 ppm disappeared and a new peak appeared at 3.35 ppm, which indicated that the hybrid membrane was successfully formed.

Microscopic morphology

The microscopic morphology of the copolymer/silica hybrid membranes was studied by SEM and TEM. The SEM images of QrP(BN/MGENB-SiO$_2$-40) are shown in Fig. 5. There were no holes on the surface and cross-section, indicating the dense nature of the obtained hybrid membrane. In addition, some dots could be attributed to silica particles on the surface of the membrane, and enhancements of the mechanical and thermal stabilities were facilitated by the addition of TSPCA.

TEM images of QrP(BN/MGENB-SiO$_2$-y) (y = 10, 20, 30 and 40 in wt% TSPCA) are shown in Fig. 6. The dark evenly-distributed nano-sized spots in the images represent the hydrophilic domains containing aggregated Si–O–Si and C–O–Si, while the bright areas represent the hydrophobic domains composed of rPNB main chains.

Fig. 6(b–d) provide direct evidence of the biphasic morphology of the copolymer/silica hybrid membranes, the TEM images exhibit a clear hydrophilic–hydrophobic microphase separation with wormlike interconnected hydrophilic network nano-channels. With increasing TSPCA, the hybrid membrane showed a darker and uniform hydrophilic domain with a small degree of connectivity. EDX spectroscopy was used to analyze the dark globular domains in one of the hybrid membranes (Fig. 6(e)), the presence of Si demonstrates the existence of TSPCA in the hybrid membrane, and the disappearance of nitrogen implies that the quaternary ammonium groups were dispersed around the hole and nanosized channels.

Thermal stability and mechanical properties

TGA curves of the copolymer/silica hybrid membranes QrP(BN/MGENB-SiO$_2$-y) are shown in Fig. S3.† Three steps of weight loss were observed: the loss of water and solvent from the hybrid membrane phase within the range of 0–120 °C, the loss of quaternary ammonium groups and the decomposition of C–O–C within the range of 120–450 °C, and the loss of membrane matrix and the degradation of Si–O–Si within the range of 450–650 °C.

Tensile curves of the copolymer/silica hybrid membranes QrP(BN/MGENB-SiO$_2$-y) are shown in Fig. S4,† and the mechanical properties are presented in Table 1. The QrP(BN/MGENB-SiO$_2$-30) hybrid membrane showed better mechanical properties than the others: the tensile strength of the hybrid membrane was 8.2 MPa and the elastic modulus was 20.4 MPa.
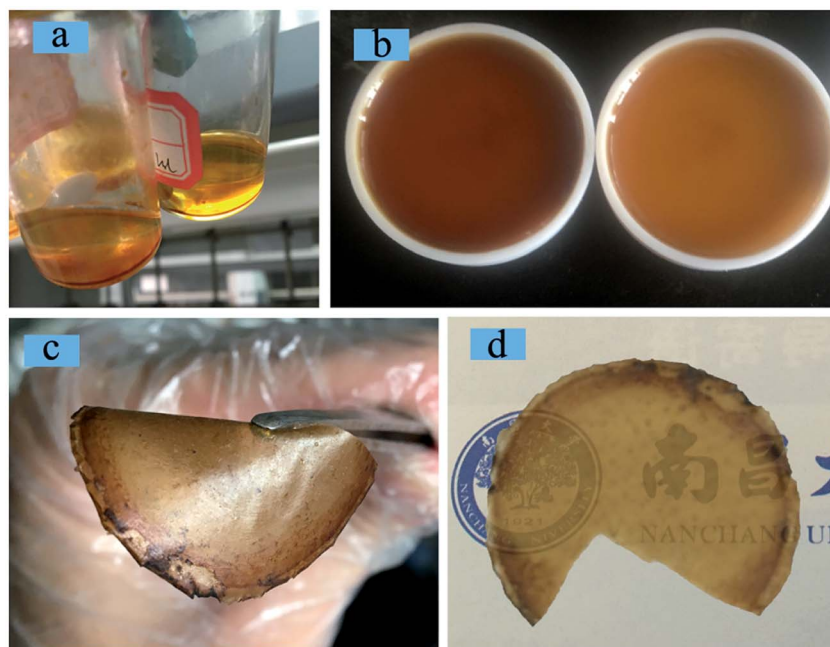
Fig. 4 Photos of copolymer/silica hybrid membranes demonstrating their (a) solubility, (b) casting, (c) flexibility, and (d) transparency.

These results indicate that the degree of cross-linking had a great influence on the mechanical properties. In the hybrid membrane materials with a low degree of cross-linking, the mechanical properties were enhanced by an order of magnitude compared to the compositions with more TSPCA. Nevertheless, a high degree of cross-linking would make the material crumbly and weaken the compression strength, therefore, the elongation at break of QrP(BN/MGENB-SiO$_2$-40) decreased remarkably, while the tensile strength at break and elastic modulus of QrP(BN/MGENB-SiO$_2$-40) were weakened slightly.

Water uptake and methanol permeability

The water uptake and methanol permeability of the copolymer/silica hybrid membranes are collated in Table 2. The hybrid membrane QrP(BN/MGENB-SiO$_2$-10) showed better water uptake (26%) than the others, and the hybrid membrane QrP(BN/MGENB-SiO$_2$-40) showed better methanol resistance permeability (1.54 × 10^{-7} cm^2 s^{-1}) than the others. The reason was that the cross-linking structure in the hybrid membranes

had a great influence on the water uptake and methanol permeability. Hybrid membranes with more TSPCA could achieve a higher degree of cross-linking and relatively compact molecular structures, which restrained the mobility of methanol as well as maintaining a lower water content in the membranes. Thus, the water uptake and methanol permeability of the hybrid membranes decreased as the TSPCA content increased from 10% to 40%.

Ion-exchange capacity, ionic conductivity and alkaline stability

The thickness, ion-exchange capacity (IEC), and ionic conductivity of the copolymer/silica hybrid membranes are also shown in Table 2. The QrP(BN/MGENB-SiO$_2$-10) showed a better IEC (1.61 × 10^{-3} mol g^{-1}) and ionic conductivity (9.7 × 10^{-3} S cm^{-1}) at room temperature than the others. The data in Table 2 indicates that the IEC and ionic conductivity of the hybrid membranes depended on the activity of the quaternary ammonium group rather than on the number of the quaternary
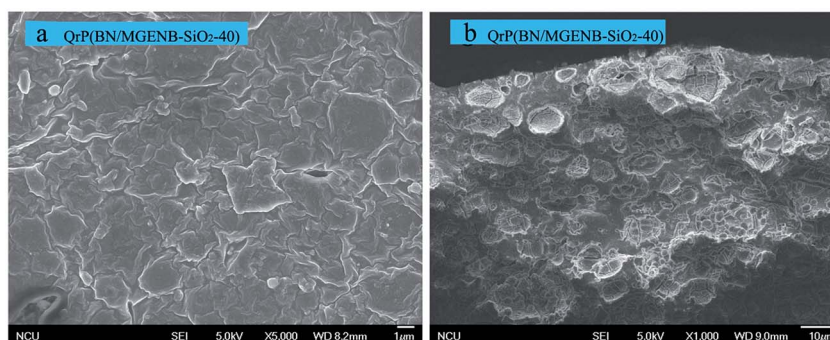

Fig. 5 SEM images of a copolymer/silica hybrid membrane: (a) SEM surface (1 μm), and (b) SEM cross-section (10 μm).
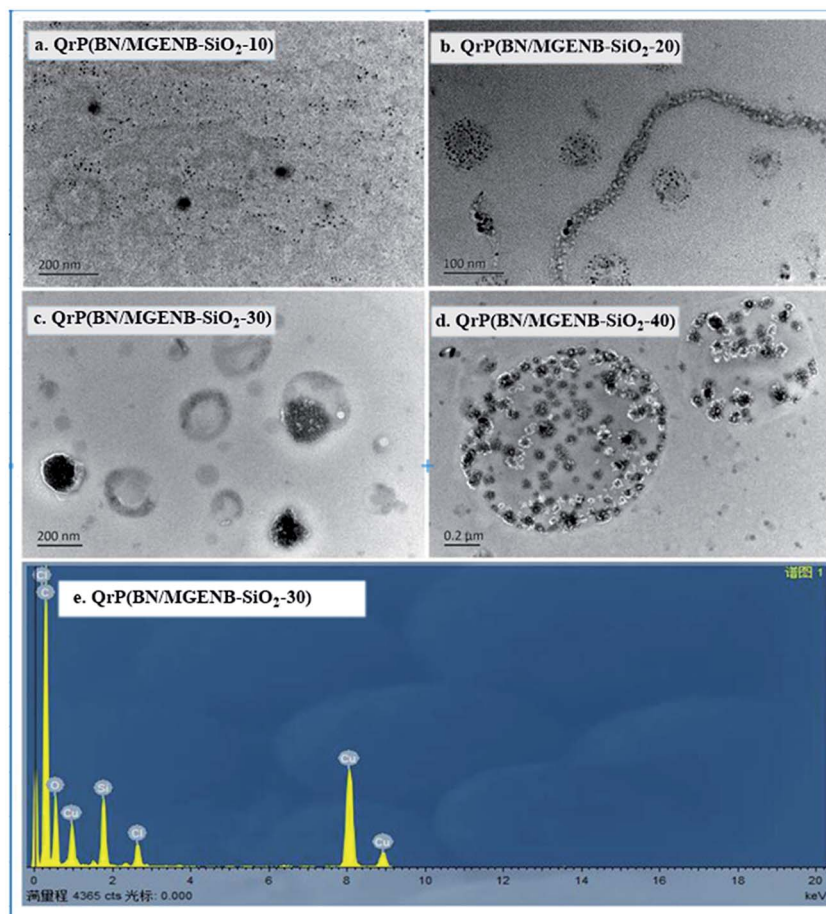
Fig. 6 TEM images of copolymer/silica hybrid membranes: (a) QrP(BN/MGENB-SiO$_2$-10), (b) QrP(BN/MGENB-SiO$_2$-20), (c) QrP(BN/MGENB-SiO$_2$-30), (d) QrP(BN/MGENB-SiO$_2$-40), and (e) the EDX spectrum of QrP(BN/MGENB-SiO$_2$-30).

ammonium groups in the hybrid membranes. The cross-linked membranes showed lower conductivity compared to the corresponding pristine ones, which might be due to two factors: (1) the relatively compact molecular structures restrained the mobility of OH$^-$ and led to lower water content in the membranes; (2) the membranes that contained cross-linking quaternary ammonium groups showed better separation of the hydrophilic domains. Therefore, the ion-exchange capacity of the hybrid membranes decreased gradually.

TSPCA was introduced into rP(BN/MGENB)-49.2 to generate a cross-linked structure, which caused the ionic conductivity to increase rapidly. The cross-linking network affected the ionic conductivity by inhibiting the water absorption (Table 2) and changing the nanophase structure in the hybrid membrane. As

can be seen in Fig. 7, the ionic conductivity of QrP(BN/MGENB-SiO$_2$-10) increased from 9.7×10^{-3} to 41.0×10^{-3} S cm^{-1} when the temperature increased from 30 to 80 °C. More quaternary ammonium groups would facilitate the transport of hydroxide and moderate water retention ability resulting from the silicon dioxide structure. This might be the key factor for the observed variations in the ionic conductivity values.

The alkaline stability of the copolymer/silica hybrid membranes was studied by soaking the membranes in a 6 M NaOH aqueous solution at 60 °C and measuring the changes in the normalized hydroxide conductivity every 24 h, and the results are shown in Fig. 8. After being soaked in the 6 M NaOH for 144 h at 60 °C, the ionic conductivity of the hybrid membranes declined in varying degrees. Compared to the other

Table 1 The major mechanical properties of the copolymer/silica hybrid membranes

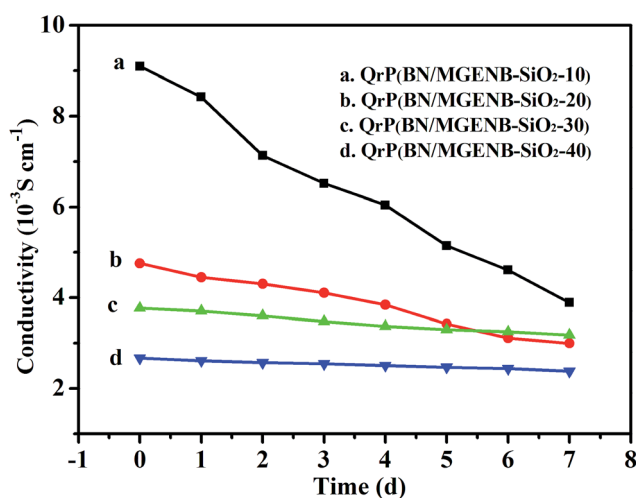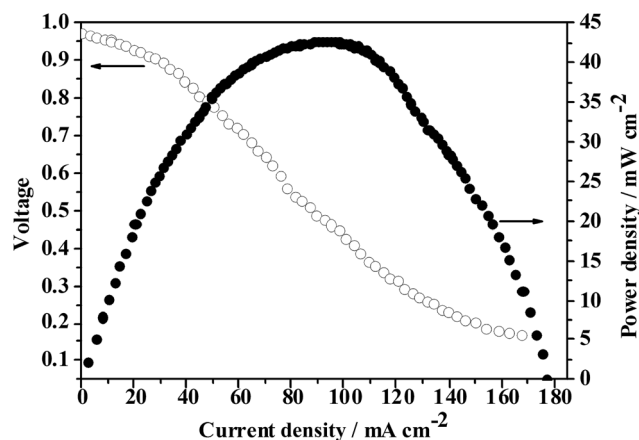| Sample	Tensile strength at break (MPa)	Elongation at break (%)	Elastic modulus (MPa)
QrP(BN/MGENB-SiO$_2$-10)	0.8	33.4	7.1
QrP(BN/MGENB-SiO$_2$-20)	1.5	44.6	10.3
QrP(BN/MGENB-SiO$_2$-30)	8.2	101.1	20.4
QrP(BN/MGENB-SiO$_2$-40)	4.9	45.7	13.4

Table 2 The thickness, water uptake (%), methanol permeability, IEC, and ionic conductivity of the copolymer/silica hybrid membranes[a]

Membrane	Water uptake (%)	Methanol permeability (10^{-7} cm^2 s^{-1})	IEC (10^{-3} mol g^{-1})	Conductivity (10^{-3} S cm^{-1})
QrP(BN/MGENB-SiO$_2$-10)	26.0	2.75	1.61	41.0
QrP(BN/MGENB-SiO$_2$-20)	24.0	2.45	1.25	34.7
QrP(BN/MGENB-SiO$_2$-30)	12.0	1.88	0.96	8.7
QrP(BN/MGENB-SiO$_2$-40)	8.0	1.54	0.94	6.3

[a] The thickness of the hybrid membranes was 0.16 mm, and the ionic conductivity was tested at 80 °C.
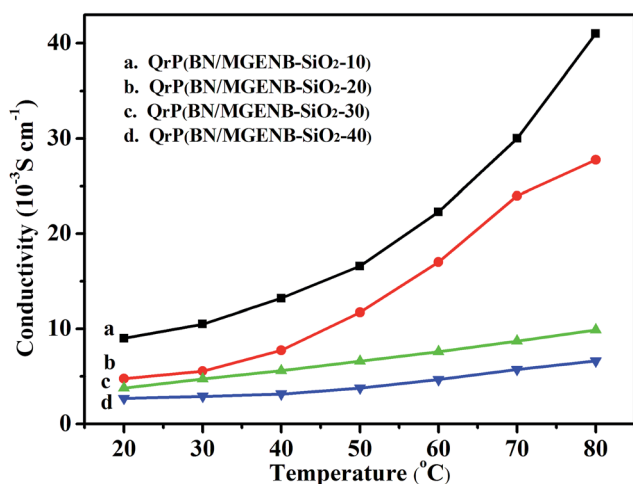
Fig. 7 The ionic conductivity of the copolymer/silica hybrid membranes at different temperatures: (a) QrP(BN/MGENB-SiO$_2$-10), (b) QrP(BN/MGENB-SiO$_2$-20), (c) QrP(BN/MGENB-SiO$_2$-30), and (d) QrP(BN/MGENB-SiO$_2$-40).

Fig. 9 Single cell performances of a MEA fabricated with the copolymer/silica hybrid membrane QrP(BN/MGENB-SiO$_2$-10).

hybrid membranes, the ionic conductivity decrease of QrP(BN/MGENB-SiO$_2$-10) was the largest, which indicated that the QrP(BN/MGENB-SiO$_2$-10) hybrid membrane had low stability in alkaline media. Meanwhile, the alkaline stability of the hybrid

membranes with higher TSPCA compositions was enhanced by an order of magnitude compared to those with lower TSPCA compositions. The cross-linked structure had a significant effect on the alkaline stability of the hybrid membranes, however, it hampered the development of the ionic conductivity simultaneously.

Single cell performance

QrP(BN/MGENB-SiO$_2$-10) was used as a representative case to be tested with a DMFC test system, and the results are shown in Fig. 9. As can be seen, the hybrid membrane QrP(BN/MGENB-SiO$_2$-10) exhibited an open circuit voltage (OCV) of 0.95 V, and a current density of 96.7 mA cm^{-2} at a peak power density of 42.6 mW cm^{-2}.

Conclusions

A series of ROMP-type epoxy-functionalized norbornene copolymers were achieved and characterized. rP(BN/MGENB)-49.2 showed better M_w and processing performance than the other copolynorbornenes. Copolymer/silica hybrid membranes were obtained *via* a sol–gel method and a solution casting method. The obtained copolymer/silica hybrid membranes exhibited low methanol permeability, good alkaline stability, high temperature stability, and good ionic conductivity and IEC. The hybrid membrane QrP(BN/MGENB-SiO$_2$-10) showed comprehensive properties: the IEC reached 1.61×10^{-3} mol g^{-1} and the ionic

Fig. 8 The alkalinity stability of the copolymer/silica hybrid membranes: (a) QrP(BN/MGENB-SiO$_2$-10), (b) QrP(BN/MGENB-SiO$_2$-20), (c) QrP(BN/MGENB-SiO$_2$-30), and (d) QrP(BN/MGENB-SiO$_2$-40).

conductivity reached 41×10^{-3} S cm^{-1} at 80 °C. The single cell performance of the MEA fabricated using QrP(BN/MGENB-SiO$_2$-10) was tested in a DMFC and it showed a maximum open circuit voltage of 0.95 V and a current density of 96.7 mW cm^{-2} at a peak power density of 42.6 mW cm^{-2}.

Further work will focus on enhancing its mechanical properties and single cell performance to satisfy the requirements of AEMs for potential application in DMFCs.

Conflicts of interest

There are no conflicts to declare.

Acknowledgements

References

1 G. Merle, M. Wessling and K. Nijmeijer, *J. Membr. Sci.*, 2011, **377**, 1–35.

2 M. A. Vandiver, R. C. Benjamin, P. Zach, Li. Yifan, S. Sonke and M. K. Daniel, *J. Appl. Polym. Sci.*, 2015, **132**, 41596–41604.

3 S. C. Min, J. Y. Lee, T. H. Kim, H. Y. Jeong, H. Y. Shin, S. G. Oh and Y. T. Hong, *J. Membr. Sci.*, 2017, **530**, 73–83.

4 X. Gong, X. Yan, T. Li, X. Wu, W. Chen and G. He, *J. Membr. Sci.*, 2017, **523**, 216–224.

5 A. Filimon, A. M. Dobos and E. Avram, *J. Chem. Thermodyn.*, 2017, **106**, 160–167.

6 W. Liu, L. Liu, J. Liao, L. Wang and N. Li, *J. Membr. Sci.*, 2017, **536**, 133–140.

7 K. Emmanuel, C. Cheng, B. Erigene, A. N. Mondal, M. Hossain, M. I. Khan and T. Xu, *J. Membr. Sci.*, 2016, **497**, 209–215.

8 M. T. Kwasny and G. N. Tew, *J. Mater. Chem. A*, 2016, **5**, 1400–1405.

9 Y. Zha, M. L. Disabbmiller, Z. D. Johnson, M. A. Hickner and G. N. Tew, *J. Am. Chem. Soc.*, 2012, **134**, 4493–4496.

10 Y. Zhao, L. Feng, J. Gao, Y. Zhao, S. Wang, V. Ramani, Z. Zhang and X. Xie, *Int. J. Hydrogen Energy*, 2016, **41**, 16264–16274.

11 B. Qiu, B. Lin, L. Qiu and F. Yan, *J. Mater. Chem.*, 2011, **22**, 1040–1045.

12 Z. Li, X. He, Z. Jiang, Y. Yin, B. Zhang, G. He, Z. Tong, H. Wu and K. Jiao, *Electrochim. Acta*, 2017, **4**, 486–494.

13 N. U. Afsar, J. Miao, A. N. Mondal, Z. Yang, D. Yu, B. Wu, K. Emmanuel and L. Ge, *Sep. Purif. Technol.*, 2016, **164**, 63–69.

14 B. Bauer, H. Strathmann and F. Effenberger, *Desalination*, 1990, **79**, 125–144.

15 W. R. Bowen and H. Mukhtar, *J. Membr. Sci.*, 1996, **112**, 263–274.

16 S. C. Price, X. Ren, A. M. Savage and L. Beyer, *Polym. Chem.*, 2017, **8**, 5708–5717.

17 X. He, J. Liu, H. Zhu, Y. Zheng and D. Chen, *RSC Adv.*, 2015, **5**, 63215–63225.

18 J. Deng, H. Y. Gao, F. M. Zhu and Q. Wu, *Organometallics*, 2013, **32**, 4507–4515.

19 S. Liu, Z. Yao and K. Cao, *J. Appl. Polym. Sci.*, 2009, **112**, 2493–2496.

20 Z. W. You, W. Song, S. Zhang, O. Y. Jin and M. R. Xie, *J. Polym. Sci., Part A: Polym. Chem.*, 2013, **51**, 4786–4795.

21 T. J. Clark, N. J. Robertson, H. A. Kostalik, E. B. Lobkovsky, P. F. Mutolo, H. D. Abruria and G. W. Coates, *J. Am. Chem. Soc.*, 2009, **131**, 12888–12889.

22 N. Saba, A. Safwan, M. L. Sanyang, F. Mohammad, M. Pervaiz, M. Jawaid, O. Y. Alothman and M. Sain, *Int. J. Biol. Macromol.*, 2017, **102**, 822–828.

23 B. Holubova, Z. Z. Cilova, I. Kucerova and M. Zlamal, *Prog. Org. Coat.*, 2015, **88**, 172–180.

24 A. T. Sunny, M. Mozetic, G. Primc, S. Mathew and S. Thomas, *Compos. Sci. Technol.*, 2017, **146**, 34–41.

25 Y. Hu, G. Du and N. Chen, *Compos. Sci. Technol.*, 2016, **124**, 36–43.

26 R. Vinodh, M. Purushothaman and D. Sangeetha, *Int. J. Hydrogen Energy*, 2011, **36**, 7291–7302.

27 X. G. Zhao, E. M. Jin, J. Y. Park and H. B. Gu, *Compos. Sci. Technol.*, 2014, **103**, 100–105.

28 S. Sang, J. Zhang, Q. Wu and Y. Liao, *Electrochim. Acta*, 2007, **52**, 7315–7321.

29 P. N. Venkatesan and S. Dharmalingam, *J. Membr. Sci.*, 2015, **492**, 518–527.

30 J. Wang, X. He, H. Zhu and D. Chen, *RSC Adv.*, 2015, **5**, 43581–43588.

31 R. M. Huertas and M. C. Fraga, *Sep. Purif. Technol.*, 2017, **180**, 69–81.

32 S. H. Liu, M. Liu, Z. L. Xu, Y. M. Wei and X. Guo, *J. Membr. Sci.*, 2017, **528**, 303–315.

33 R. Nistico, D. Scalarone and G. Magnacca, *Microporous Mesoporous Mater.*, 2017, **248**, 18–29.

34 Q. Zhang, J. Jiang, F. Gao, G. Zhang, X. Zhan and F. Chen, *Chem. Eng. J.*, 2017, **321**, 412–423.

35 L. Zhu, H. Song, J. Wang and L. Xue, *Mater. Sci. Eng., C*, 2017, **74**, 159–166.

36 S. F. Liu, Y. W. Chen, X. H. He, L. Chen and W. H. Zhou, *J. Appl. Polym. Sci.*, 2011, **121**, 1166–1175.